

## EXPERIMENTAL FORMATION OF A MICROBIAL DEATH MASK

SIMON A.F. DARROCH,<sup>1</sup> MARC LAFLAMME,<sup>1,2\*</sup> JAMES D. SCHIFFBAUER,<sup>3,4</sup> and DEREK E.G. BRIGGS<sup>1,5</sup>

<sup>1</sup>Department of Geology and Geophysics, Yale University, PO Box 208109, New Haven, Connecticut 06520-8109, USA, [simon.darroch@yale.edu](mailto:simon.darroch@yale.edu); <sup>2</sup>Current address: Smithsonian Postdoctoral Fellow, Department of Paleobiology, MRC-121, National Museum of Natural History, Washington, D.C. 20013-7012, USA, [laflamme@si.edu](mailto:laflamme@si.edu); <sup>3</sup>Nanoscale Characterization and Fabrication Laboratory, Institute for Critical Technology and Applied Science, Virginia Polytechnic Institute and State University, Blacksburg, Virginia 24061, USA, [jdschiffbauer@gmail.com](mailto:jdschiffbauer@gmail.com); <sup>4</sup>Department of Geosciences, Virginia Polytechnic Institute and State University, Blacksburg, Virginia 24061, USA; <sup>5</sup>Peabody Museum of Natural History, Yale University, P.O. Box 208118, New Haven, Connecticut 06520-8118, USA, [derek.briggs@yale.edu](mailto:derek.briggs@yale.edu)

## ABSTRACT

This study represents a first attempt to observe soft-tissue decay in association with microbial mats, in order to recreate the death-mask model proposed for terminal Neoproterozoic Lagerstätten. This model explains the precipitation of authigenic iron sulfide minerals on, and around, decaying carcasses in association with microbial mats, cementing the sediment as a sole veneer and retaining the external morphology of the organism in relief on the upper and lower surface of coarse-grained sandy event beds. Although this model has been substantiated by the discovery of abundant microbially induced sedimentary structures (MISS) and pyrite veneers in close association with Ediacaran fossils, it has not been tested previously by experimental taphonomic studies under controlled laboratory conditions. Arthropod larvae that decayed on top of a cyanobacterial mat demonstrated higher quality preservation of fine-scale anatomy than larvae that decayed in the absence of a mat. Decay experiments involving bacterial mats and organic-rich sands generated a black ring extending radially from the decaying carcasses. When this precipitate was analyzed using XPS and ESEM-EDS it revealed the presence of likely iron sulfides, or at least spatially associated Fe and S, and localized concentrations of common aluminosilicate elements (Al, K, Fe, and Mg), which is a composition that has been documented in association with Ediacaran fossil preservation.

## INTRODUCTION

Taphonomic experiments under controlled laboratory conditions have played a pivotal role in exploring the chemical and physical influences on organismal decay and the preservation of fossils (Briggs, 1995, 2003). Physicochemical controls can be investigated systematically in order to distinguish causes from consequences, thereby assisting in the interpretation of death, decay, and diagenesis (Allison, 1988; Briggs, 1995). Sansom et al. (2010) demonstrated that in some groups, decay can compromise taxonomic identification; understanding organismal decay rates and patterns, therefore, is crucial to interpreting biological affinity. The various physical and chemical processes leading to preservation of labile soft tissues continue to be studied (Briggs, 2003). Taphonomic investigations of modern organisms can contribute significantly to our understanding of extinct groups (e.g., Briggs and Kear, 1994). However, there are invariably more enigmatic soft-bodied fossils awaiting taphonomic investigation than there are workers pursuing such research. Nowhere is this deficiency more striking than in the case of the enigmatic Ediacaran organisms (Xiao and Laflamme, 2009).

The Ediacara biota represents a polyphyletic group of soft-bodied organisms that was distributed worldwide in the latest Neoproterozoic. Phylogenetic relationships among and within the Ediacara biota are contentious, due, at least in part, to taphonomic features that have yet

to be investigated in the laboratory. Over the course of ~60 years of study, various Ediacaran organisms have been allied with cnidarians (Sprigg, 1949), stem- (Fedonkin and Waggoner, 1997; Sperling et al., 2007) and crown-group (Glaessner and Wade, 1966; Gehling, 1991; Sperling and Vinther, 2010) metazoans, lichens and fungi (Retallack, 1994), or placed in an extinct kingdom or phylum—the Vendozoa/Vendobionta (Seilacher, 1989, 1992). An increasing body of evidence suggests that the Ediacara biota represents a diversity of unrelated organisms sharing a common mode of preservation (Narbonne, 2005; Xiao and Laflamme, 2009; Erwin et al., 2011). Central to this taphonomic scenario is the microbial death-mask model proposed by Gehling (1999; see below). This model emphasizes the role played by sulfur-reducing bacteria in precipitating iron sulfide minerals, which in turn ultimately form mineralized, pyritic death masks around carcasses.

## HISTORY OF EDIACARAN EXPERIMENTAL TAPHONOMY AND THE MICROBIAL DEATH-MASK MODEL

Early taphonomic experiments by Norris (1989) and Bruton (1991) attempted to simulate Ediacara-type preservation of soft-bodied organisms, but their experiments were restricted largely to cnidarians and did not incorporate microbial mats in the experimental design. Norris (1989) devised a series of protocols to target scyphozoans and pennatulids. However, even with instant burial and lithification, only simple structures were replicated and organisms under 3–4 cm in diameter were not preserved (Norris, 1989). These results are at odds with the Ediacaran fossil record, which includes numerous taxa with well-defined structures smaller than this 3–4 cm threshold (Clapham et al., 2003; Narbonne, 2004; Droser et al., 2006; Narbonne et al., 2009). Buried pennatulids almost invariably became distorted in Norris's (1989) experiments (much more so than morphologically comparable Ediacaran fronds; see Laflamme and Narbonne, 2008), prompting him to argue that the integument in Ediacaran organisms must have been substantially stiffer or more recalcitrant than in extant cnidarians. These experiments also demonstrated the importance of organic compounds in controlling the fidelity of preservation: specimens buried in clean (i.e., with organic content removed) sands immersed in seawater decayed completely within a week of burial without leaving any recognizable impressions; identical specimens buried in organic-rich sand produced excellent impressions, stabilized by the persistence of an organic membrane.

Bruton (1991) conducted experimental studies on stranded jellyfish. He noted that cast-and-mold-type preservation could occur where jellyfish were washed ashore and desiccated on a beach strandline, while taphonomic experiments conducted using the same jellyfish submerged in water did not produce any impressions due to their virtually neutral buoyancy. However, the results achieved on strandlines may not be relevant to any known Ediacaran localities, as they are all interpreted as representing subtidal paleoenvironments (Narbonne, 1998; Gehling, 2000; Grazhdankin, 2004; Wood et al., 2003; Wilby et al., 2011). This

\* Corresponding author.

Published Online: May 2012

diminishes the likelihood of desiccation prior to fossilization (Gehling, 1991; Briggs, 1995). Even though they failed to replicate the nature of Ediacaran fossils, the experiments by Norris (1989) and Bruton (1991) showed that the Ediacaran taphonomic window involved more than simple burial of metazoans by storm events.

Gehling (1999) was the first to propose that Ediacaran-type preservation was not simply controlled by biological factors of the preserved organism, such as integument strength, but also relied on external agents—principally the role of microbial mats in generating extracellular polymeric substances (or exopolysaccharides, EPS). In the absence of effective metazoan grazing and bioturbation, thick microbial mats accumulated in normal, shallow-marine settings (Seilacher, 1984), thus isolating dysoxic-anoxic pore waters from the oxygenated water above the sediment-water interface. Under these conditions, sulfate-reducing bacteria (SRBs) converted sulfate ( $\text{SO}_4^{2-}$ ) to hydrogen sulfide ( $\text{H}_2\text{S}$ ), which in turn combined with iron in pore water to form a pyritic ( $\text{FeS}_2$ ) death mask around buried and decaying organisms (Gehling, 1999; Gehling et al., 2005).

The death-mask model predicts that, following the rapid burial of benthic Ediacaran communities (along with associated microbial mats), a new mat will colonize the top of the storm layer and new sediment-water interface, sealing off the underlying sediment from dissolved gas transport. Following the collapse of labile tissues and subsequent compaction, sediment fills the voids in the underlying bacterial mat, forming a positive structure on the base of the bed (positive hyporelief). Organisms with more recalcitrant integument, on the other hand, resist decay for significantly longer (days to weeks), allowing SRB-generated  $\text{H}_2\text{S}$  to precipitate iron sulfides that coat the outer surface of the organisms, resulting in a void in the overlying sediment (negative hyporelief). Uncemented sediment from below is pushed upward into the cavity left when the organism decayed, forming a cast of the upper surface of the organism on the underlying bed (positive epirelief; see Gehling, 1999, fig. 11).

The death-mask hypothesis is supported by a number of lines of evidence: (1) Partings associated with fossiliferous horizons in the Flinders Ranges commonly are stained with hematite and limonite, both interpreted as weathering products of pyrite that formed in association with anaerobic decay of organisms and associated microbial mats (Gehling, 1999; Callow and Brasier, 2009). (2) Microbial textures (e.g., *Kinnevia*- and *Arumberia*-type wrinkle structures) and microbially induced sedimentary structures (MISS) are common in beds that preserve Ediacaran fossils (Hagadorn and Bottjer, 1997; see table 1 in Gehling, 1999; Laflamme et al., 2012). In the Flinders Ranges, these structures are useful indicators of the position of fossiliferous beds in the field (Gehling, 1999). In rare cases microbial filaments are preserved in pyrite on bedding surfaces, most spectacularly in the fossilized mats from the White Sea locality (Fedonkin and Waggoner, 1997; Steiner and Reitner, 2001; Gehling et al., 2005; Grazhdankin and Gerdes, 2007; Callow and Brasier, 2009). (3) Pyrite framboids and iron oxide pseudomorphs have been found in direct association with three-dimensionally preserved *Aspidella* holdfasts (Laflamme et al., 2011). (4) Ediacaran fossils from the Windermere Supergroup, northwestern Canada, are associated with carbonaceous partings suggestive of organic rich substrates (Narbonne, 1998). (5) A significant number of Phanerozoic localities preserving soft tissues also reveal the presence of microbial mats or bacterial biofilms (e.g., Wilby et al., 1996), in particular Lower Cretaceous limestone units at Las Hoyas, Spain (Gupta et al., 2008), and the beds that yield exceptionally preserved vertebrate tissues at Libros, Spain (McNamara et al., 2009).

Narbonne (2005) outlined four distinct pathways that account for most of the variability in the preservation of Ediacaran fossils: (1) Conception-type preservation: fossils in positive and negative epirelief cast by volcanic ash, (2) Nama-type preservation: three-dimensional fossils within event beds, (3) Flinders-type preservation: fossils in positive and negative hyporelief in shallow marine settings, and (4)

Fermeuse-type preservation: fossils in negative hyporelief in deep marine settings. Narbonne (2005) invoked the influence of bacterial mats for Flinders-type preservation, and suggested that deep-water heterotrophic mats were likely responsible for Fermeuse- and, to a lesser degree, Conception-type preservation. However, the influence of bacterial mats on the preservation of both gross morphology and labile tissues remained to be demonstrated in the laboratory. Liu et al. (2011) suggested that several Ediacaran forms from Newfoundland are in reality taphomorphs brought about by postmortem microbial decay, (although see Wilby et al., 2011; Laflamme et al., 2012), bringing many interpretations of census diversity and paleoecology into question. Taphonomic experiments involving microbial mats represent an opportunity to test these hypotheses.

## MATERIALS AND METHODS

### Study Organisms

The larva of *Galleria mellonella* (Lepidoptera; Pyralidae) used for decay experiments were chosen for their relatively simple external morphology, which allowed simple quantification of taphonomic state and stages. *G. mellonella* larvae are well studied and frequently used in scientific research as model organisms (e.g., Miyata et al., 2003). In particular, the responses of *G. mellonella* cuticle to enzymatic hydrolysis are well known (Samsinakova et al., 1971; Gupta et al., 1992, 1994). All larvae were 1–2 cm in length, purchased from commercial pet stores, and alive at the start of experimentation.

### Mats

Mats were collected from freshwater ponds of the North Branford Traprock Quarry, Connecticut (41°30'51.12"N, 73°12'56.03"W). After collection, they were incubated in tanks for a minimum of 6 months; light was administered in diurnal 12-hour cycles, and tap water was added to prevent desiccation. The top ~0.5 cm of the mat was coherent and easily peeled away from the silty substrate on the quarry floor. The underside of the mat revealed dense pitting presumably resulting from gas generation at the mat-sediment interface. An intense color zonation developed over the course of several weeks' incubation in the laboratory, which represented depth-related zonation of microbial metabolic processes and associated redox boundaries. Centimeter-scale fenestrae developed after 2 weeks, typically elongate parallel to the surface. The upper surfaces of mats became wrinkled, and in some cases large gas bubbles were evident trapped at the mat-water interface.

DNA extraction, bacteria-specific 16S PCR, and cloning were performed on mat samples (methods outlined in Supplementary Data 1<sup>1</sup>). The bacterial community sequences from the mat sample are shown in a phylogenetic tree (Supplementary Data 2<sup>1</sup>), and are compared with sequences entered in the Ribosomal Database Project (Cole et al., 2009). Overall, microbial diversity at this site was high; bacteria from our clone library had good matches with Acidobacteria, Betaproteobacteria, Cyanobacteria, Planctomycetes, Verrucomicrobia, Spingobacteria, and Deltaproteobacteria (see Supplementary Data 1<sup>1</sup>). These matches agree well with expectations of the types of organisms found in the microbial mat we sampled. Mats were also observed to host a diverse meiofauna of ostracodes and diatoms.

### Experimental Procedure

Small (~3 cm<sup>2</sup>) patches of mat were placed in shallow glass dishes (Fig. 1) and left to settle for 2 hours under tap water. The composition of this water was determined by ion chromatography (Supplementary Data 3<sup>1</sup>). Larvae of *G. mellonella* were killed by crushing the head with forceps.

<sup>1</sup> palaios.ku.edu.

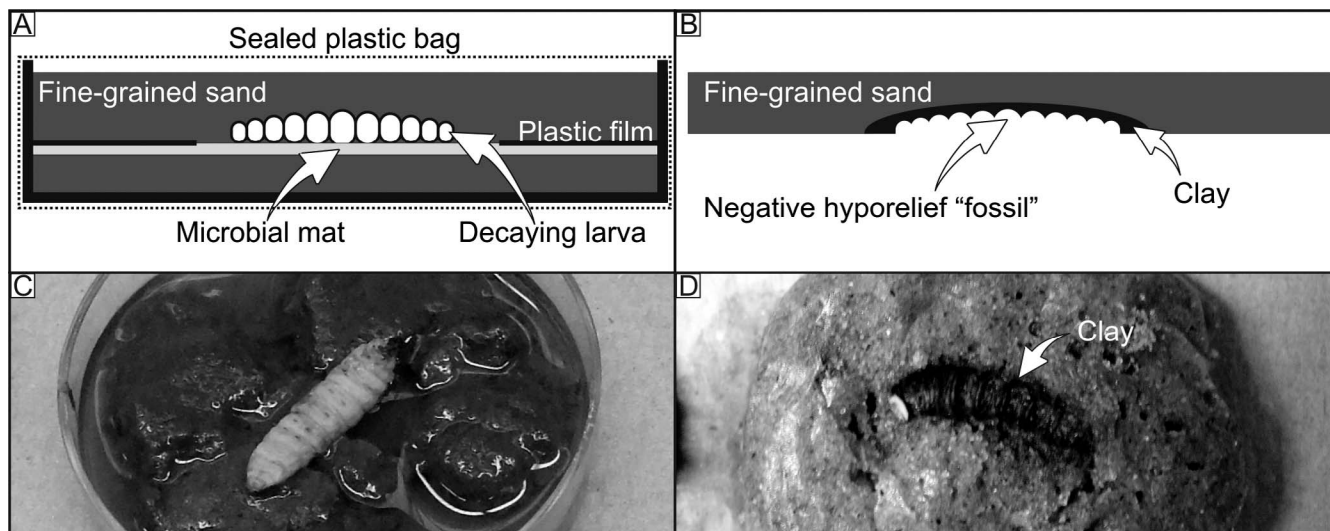


**FIGURE 1**—Experimental protocol. A) Fine-grained (250–125  $\mu\text{m}$ ) sand was packed in the bottom of a glass petri dish and covered by a thin (<1 cm) microbial mat. A dead larva was placed in the center of the mat (as shown in C). A clear plastic film was placed over the mat, with a hole cut around the larva and a portion of the mat immediately surrounding it, and subsequently covered by fine-grained sand. Experiments were contained within sealed plastic bags to limit contamination. B) Idealized cross section through the negative hyporelief “fossil” mold in the bottom of the overlying bed, with the dark black rind as shown in (D).

Freshly killed individuals were then placed on top of the mat, and excess water pipetted off so that <1 mm remained. In order to facilitate removal and splitting for sampling, sheets of plastic film (standard store-bought food wrap) were placed at the bottom of dishes and on the tops of mats, with a circle cut out to allow contact between larva and mat (in the manner of Norris, 1989). Sand was layered carefully on top, taking care not to flatten or deform the carcass. The sand was collected from the strandline at Lighthouse Point Beach, New Haven, Connecticut (41°14'53.01"N, 72°54'13.99"W), and sieved using a graded series (#'s 5, 10, 18, 40, and 60) of mesh sizes. All sand used in experiments was limited to the fine-grained fraction (sieve #40 = 250–125  $\mu\text{m}$ ). Experiments were saturated in fresh water (until liquid was evident on top of the sand layers) and sealed in plastic bags before incubation (Fig. 1).

Two sets of control experiments were performed to test the influence of microbial mats on the fidelity of preservation. In the first set (C1) no mat was used; larvae were buried between layers of the same sand used in the mat experiments. In the second set (C2), again in the absence of a mat, the sand used was first cleaned of organic material by rinsing in 80% bleach solution for a period of 24 hours (vigorously stirred every 6–8 hours), and then washed in deionized water.

Decay experiments were incubated for a period of 6 weeks at a constant 33 °C. Experiments were sampled at intervals of 6 hours, 1 day (24 hours), 1 week (168 hours), 2 weeks (336 hours), and 6 weeks (1008 hours). Four replicate experiments were performed for each set of conditions (Mat, C1, C2), resulting in a total of 60 experiments. For sampling, experiments were removed from the incubator, frozen for 24 hours at –60 °C, and then split to reveal the decomposed larva and preserved morphology. All larval remains were carefully removed from the cavity, and the resulting impressions imaged under light microscopy. Due to the relatively high relief of the structures generated, between 9 and 25 images were taken of each example at different focal planes to incorporate the full depth of field, and these images were composited using Helicon Focus software. All the structures examined were from the underside of the overlying sand layer (negative hyporelief of Seilacher et al., 1985) so that the quality of impressions could be compared to fossils found at the Flinders Range locality where this is the most common mode of preservation. A simple taphonomic index (see below), based on the presence or absence of evidence for thoracic segments and abdominal prolegs in impressions, was used to compare the quality of preservation between experimental conditions.

#### Taphonomic Indices

Taphonomic indices have been used in previous studies as a semiquantitative method for documenting rates and patterns of decay (Briggs and Kear, 1994). The morphology of the *G. mellonella* larva allowed a series of simple decay indices to be defined. The body is segmented, with several sets of abdominal prolegs protruding from the ventral side. Carcasses were oriented with the prolegs projecting upward into overlying sand. Taphonomic indices (Fig. 2; Table 1) were defined as follows: (1) Evidence of prolegs and segments retained (exceptional); (2) Evidence of segments but no prolegs (good); (3) No structure retained although a cavity survives (poor); and (4) No indication that a larva was present. Experiments that split in a manner that prevented taphonomic quantification of the impression received a designation of not recoverable (NR).

#### Analytical Protocol

Samples were subjected to X-ray and electron microbeam analyses, including elemental surveys via X-ray photoelectron spectrometry microprobe (XPS: PHI Quantera SXM) and elemental point spectral and mapping analyses via energy dispersive X-ray spectroscopy in an environmental scanning electron microscope (ESEM-EDS: Bruker AXS Quantax 400 SDD housed in an FEI Company Quanta 600F). Samples were prepared for analysis by removing black-stained sediment proximal to the ventral side of the *G. mellonella* larval trace and spreading it onto a copper mounting medium (to aid charge dispersal and provide compositional contrast between the mounting medium and sediment grains) attached to a 1 cm<sup>2</sup> precleaned glass slide. Sediments were characterized initially via XPS using operating conditions as follows: power = 48.1 W, pass energy = 280 eV, spot size = 200  $\mu\text{m}$ , and take-off angle = 45°. The samples were then affixed to standard aluminum electron microscopy stubs and sputter-coated with 4.5–5 nm of Au-Pd (to aid further in charge dispersal) for ESEM-EDS analyses. All ESEM-EDS analyses were performed with identical operating conditions: high vacuum mode, working distance = 11.5 mm, accelerating voltage = 20 keV, spot size = 6.0, point collection time = 100 sec live time, and elemental map collection time = 20 minutes live time. For each sample, >30 EDS points were randomly assigned on separate grains (one spot per grain; Table 2). For EDS point analyses,

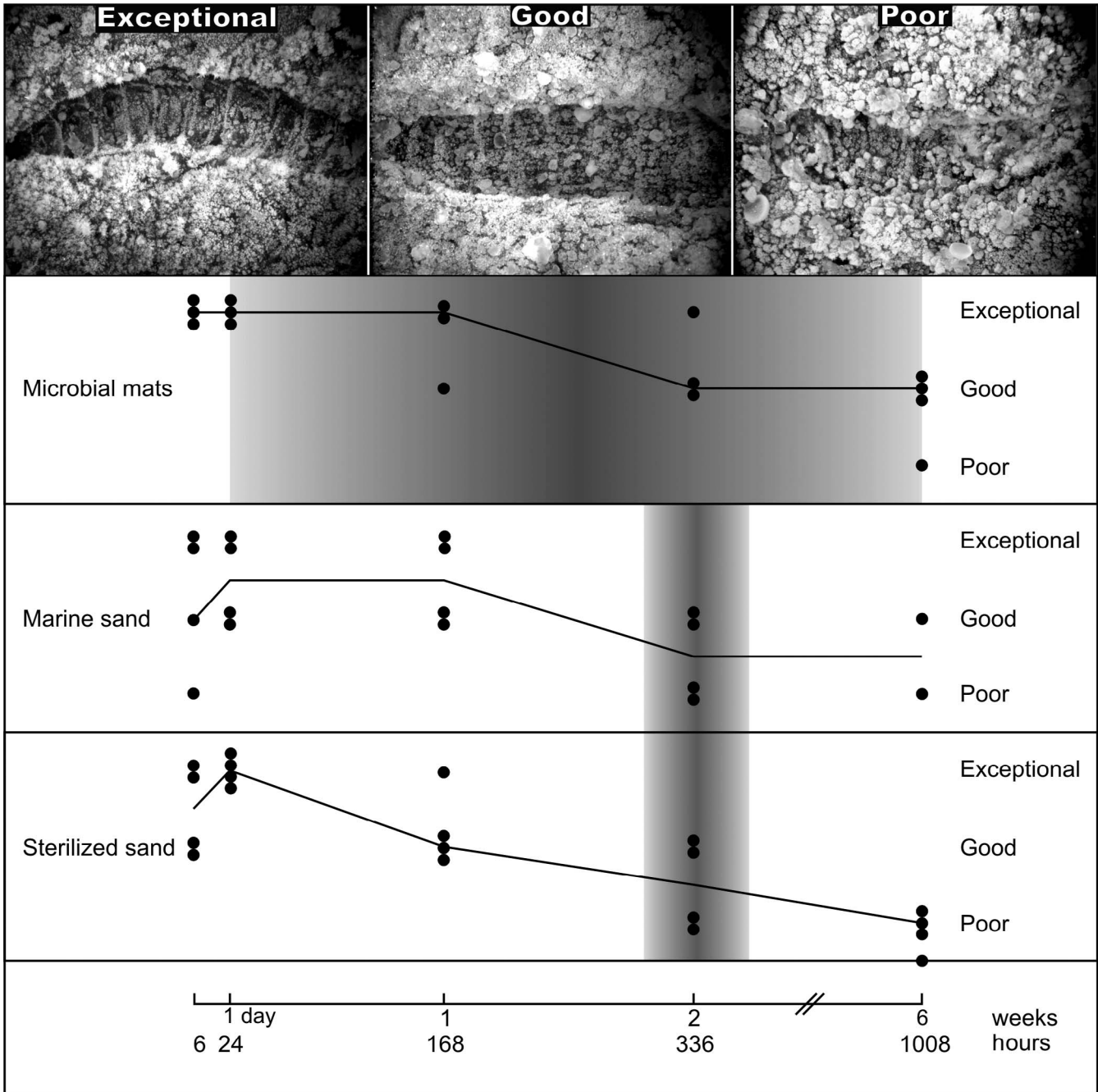


**FIGURE 2**—Results of the decay experiments. Upper frames represent the three taphonomic indices used, from exceptional (segments and prolegs), through good (segments only) to poor (general outline only). Experiments were run on three different media: microbial mats, fine-grained marine sands, and sterilized fine-grained sands. Experiments were recovered at intervals of 6 hours, 1 day (24 hours), 1 week (168 hours), 2 weeks (336 hours), and 6 weeks (1008 hours). Four replicates (black circles) were recovered at each stage for each of the three media; only 6 of 60 could not be scored. Trend lines correspond with median taphonomic index scores at each sample interval. Shaded area indicates the distribution of black precipitate, with density corresponding to prevalence of aluminosilicate precursors, and can be interpreted as a representation of the optimal window for preservation.

measures were taken to avoid potential topographic influence or variation in operating conditions, including: (1) independent adjustment of working distance to 11.5 mm between each analyzed point; (2) selection of flatter, centrally located portions of grains for placement of points (grain edges were avoided), which serves to maintain a consistent take-off angle; and (3) monitoring of X-ray signal throughout point analyses to avoid including aberrant data within the dataset (if the signal was abnormally low compared to other points, collection was immediately halted and the point was repositioned). Elemental X-ray maps may still include topographically induced artifacts, although

efforts were taken to map only regions that exhibited the least variation in grain height and size.

## RESULTS

### Recovery of Potential Fossils

90% recovery was achieved, with 54 out of 60 experiments yielding impressions that could be scored using the taphonomic index. Of the 6 examples that were not recoverable, 5 belonged to experiments

**TABLE 1**—Taphonomic indices; 3 different experimental setups were run for a period of 6 weeks, with sampling intervals at 6 hours, 1 day, 1 week, 2 weeks, and 6 weeks. Left columns indicate taphonomic index (T.I.); right columns indicate maximum distance (in mm; maximum distance from the edge of the carcass outline) reached by the black precipitate from carcass. 0 values indicate that precipitate was confined to the impression of the carcass. MAT = experiments performed with microbial mats; C1 = experiments performed with no mat and untreated sand; C2 = experiments performed with no mat and sand treated with 80% bleach solution; PPT = precipitate; NR = not recoverable.

Exp. And replicate	6 HRS		1 DAY		1 WK		2 WK		6 WK		
	T.I.	PPT	T.I.	PPT	T.I.	PPT	T.I.	PPT	T.I.	PPT	
MAT	1	1	-	1	18	2	12	1	22	2	2
	2	1	-	1	-	1	21	2	16	2	-
	3	1	-	1	-	1	9	2	16	3	0
	4	NR	-	NR	-	NR	-	NR	-	3	-
C1	1	1	-	1	-	1	-	2	16	3	-
	2	2	-	2	-	2	-	2	20	2	-
	3	3	-	1	-	1	-	3	0	NR	-
	4	1	-	2	-	2	-	3	-	NR	-
C2	1	1	-	1	-	2	-	2	6	3	-
	2	1	-	1	-	1	-	2	-	3	-
	3	2	-	1	-	2	-	3	-	3	-
	4	2	-	1	-	2	-	3	-	4	-

performed with microbial mats; sediment tended to be caked around carcasses in these experiments inhibiting splitting along laminae imposed by sheets of plastic film. Recovery became progressively more difficult with successive stages of decay: incubation for 2 weeks and beyond led to desiccation of the carcass and decay of the internal musculature, leaving a void typically lined with the remains of cuticle. After 6 weeks, carcasses had deteriorated noticeably less in experiments with mats than in either of the controls: a significant volume of both liquidized muscle tissue and cuticle remained.

#### Taphonomic Indices

Sets of experiments yielded consistent results; replicates rarely exhibited large variation in the taphonomic index (with the exception of C1, see Fig. 2). After freezing at  $-60^{\circ}\text{C}$  for a period of several days, ice crystals developed on the surface of the potential fossils which served to highlight preserved structures in a manner similar to coating with ammonium chloride powder. Impressions of abdominal prolegs (taphonomic index 1) were developed in all experiments sampled at intervals of 6 hours and 1 day (Figs. 2–3). Proleg impressions disappeared in both control experiments after 1 week, but persisted in experiments with mats up until 2 weeks. Taphonomic indices remained higher in those experiments using mats (Fig. 2): in 3 of 4 such experiments, impressions of segments were recovered after 6 weeks of decay, whereas in the control experiments the vast majority of samples preserved only the vaguest impression of the shape of the carcass (Fig. 3). Higher fidelity in the preservation of fine-scale structures was also associated with the generation of a black precipitate within and radiating outward from the void left by the decaying carcass (Fig. 1D; Fig. 4 bottom left).

#### Black Precipitate

In several experiments a ring of black precipitate formed in association with the carcass, developing first around the decaying larva, and then spreading outward along the contact between decay substrate and overlying sand. In some cases black precipitate also formed in the overlying (but rarely the underlying) sediment, resulting in a 3-dimensional black ring around the carcass (Figs. 1D, 4). Precipitate (measured as maximum distance from the edge of the

carcass outline) was most commonly and most extensively developed in experiments with mats (Table 1). This black material tended to disappear after extensive periods of decay possibly due to sulfide and/or aluminosilicate precursor oxidation following the decay of the most labile tissues (Briggs and Kear, 1994; Sagemann et al., 1999). Precipitate was formed in mat experiments after 1 day, reached a maximum extent after 2 weeks, and in one case persisted for at least 6 weeks. Precipitate also formed within 2 weeks to a more limited extent in 3 out of 4 control experiments using unsterilized sand, but none persisted. Precipitate formed in only one out of the 20 experiments using sterilized sand.

#### Chemical Composition

Three samples were analyzed via XPS and ESEM-EDS to represent the spectrum of resulting conditions: C1/6HRS (no precipitate formed; see Table 1), MAT/1WEEK (moderate precipitate formed), and C1/1WEEK (heavy precipitate formed). These are referred to below as samples 1–3 respectively. XPS elemental surveys indicated the surficial presence of C, N, O, Na, Cl, Si, Ca, and Fe in all three analyzed sediment samples. ESEM-EDS elemental mapping indicates that sediment without black precipitate (sample 1) was composed primarily of siliceous grains (Fig. 4). These analyses also illustrate a progressive dirtying of the sediment grains in samples 2 and 3 by an elemental consortium of predominantly Al, K, and Fe (i.e., an aluminosilicate-like composition) simultaneously with the formation of the black precipitate (Fig. 4). Elemental mapping of grains from sample 1 (in which no precipitate formed) showed an inverse correlation between Si, and both Al and K. EDS point data yielded mean normalized weight percentages ( $n = 31$ ) for all analyzed grains as follows: Si =  $31.2 \pm 2.0\%$ , Al =  $3.6 \pm 0.8\%$ , and K =  $0.8 \pm 0.3\%$ . In samples 2 (moderate precipitate) and 3 (heavy precipitate), Al ( $4.2 \pm 0.7\%$  and  $5.8 \pm 0.6\%$ ) and K ( $1.7 \pm 0.5\%$  and  $2.4 \pm 0.6\%$ ) became increasingly larger in concentration (Table 2; Fig. 4), and surface concentrations of Si were significantly lessened as apparent from point analyses ( $28.5 \pm 1.4\%$  and  $27.9 \pm 1.2\%$ ) and a diminished Si signal in a greater number of grains in corresponding elemental maps.

Two other common aluminosilicate elements, Mg and Fe, showed different trends. While the mean normalized weight percentages of these elements did not show a significant increase in concentration in samples 1–3 (Table 2), proportionally more grains per sample showed detectable quantities of these elements. Point analyses for sample 1 resulted in mean normalized weight percentages for Mg and Fe of  $0.7 \pm 0.3\%$  and  $1.7 \pm 0.6\%$ , respectively, and detectable quantities of both these elements were present in 52% of the analyzed grains (16 of 31 points). In sample 2, the mean Mg and Fe normalized weight percentages were  $0.8 \pm 0.2\%$  and  $2.4 \pm 0.7\%$ , and from point analyses, these elements were detectable in 57% (Mg, 26 of 46 points) and 70% (Fe, 32 of 46 points) of the analyzed grains. Sample 3 showed mean normalized weight percentages of  $0.7 \pm 0.1\%$  and  $1.8 \pm 0.7\%$  respectively for Mg and Fe, but 64% (Mg, 35 of 55 points) and 75% (Fe, 41 of 55 points) of the analyzed grains contained these elements.

Sulfur was nearly absent from sample 1 (only present in 1 analyzed point, normalized weight percentage =  $0.9\%$ ), but appeared in significant concentrations (up to  $3.7\%$  normalized weight percentage in individual spots) in samples 2 and 3 (mean normalized weight percentages of  $0.3 \pm 0.1\%$  and  $0.2 \pm 0.1\%$  respectively). In sample 1, the one S-bearing spot showed no correspondence with Fe. In samples 2 and 3, in contrast, S was always found in conjunction with points containing Fe (13% of the Fe-bearing spots [9% of total spots] in sample 2 and 17% of the Fe-bearing spots [13% of total spots] in sample 3 also contained detectable S), indicating the likely presence of iron sulfides on the surface of grains. Other elements present consistently within point analyses include Ca, Na, and Cl (in all cases, mean normalized weight percentage  $\leq 3.2\%$ ).

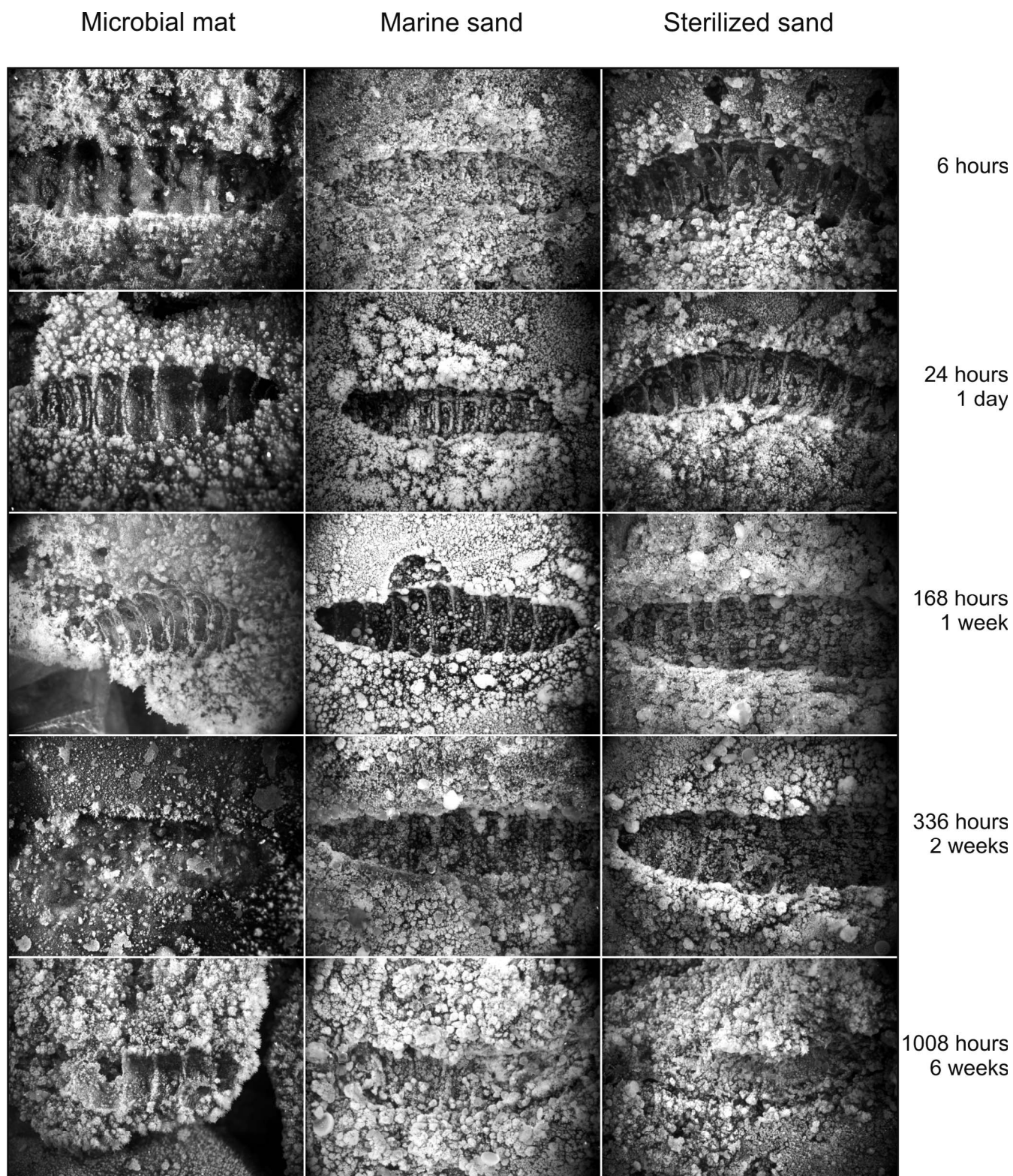


**FIGURE 3**—Decay through time: Representative samples of the negative hyporelief “fossil” molds recovered during the experiment. Samples collected between 6 hrs and 1 week were consistently better preserved (typically exceptional to good preservation) than those recovered later. Initial decay is necessary for the observed increase of aluminosilicate elements, which increased preservational potential in later (post-1-week) samples. The presence of a bacterial mat is associated with higher-quality preservation, while relatively poor preservation is achieved in sand-only samples after one week.

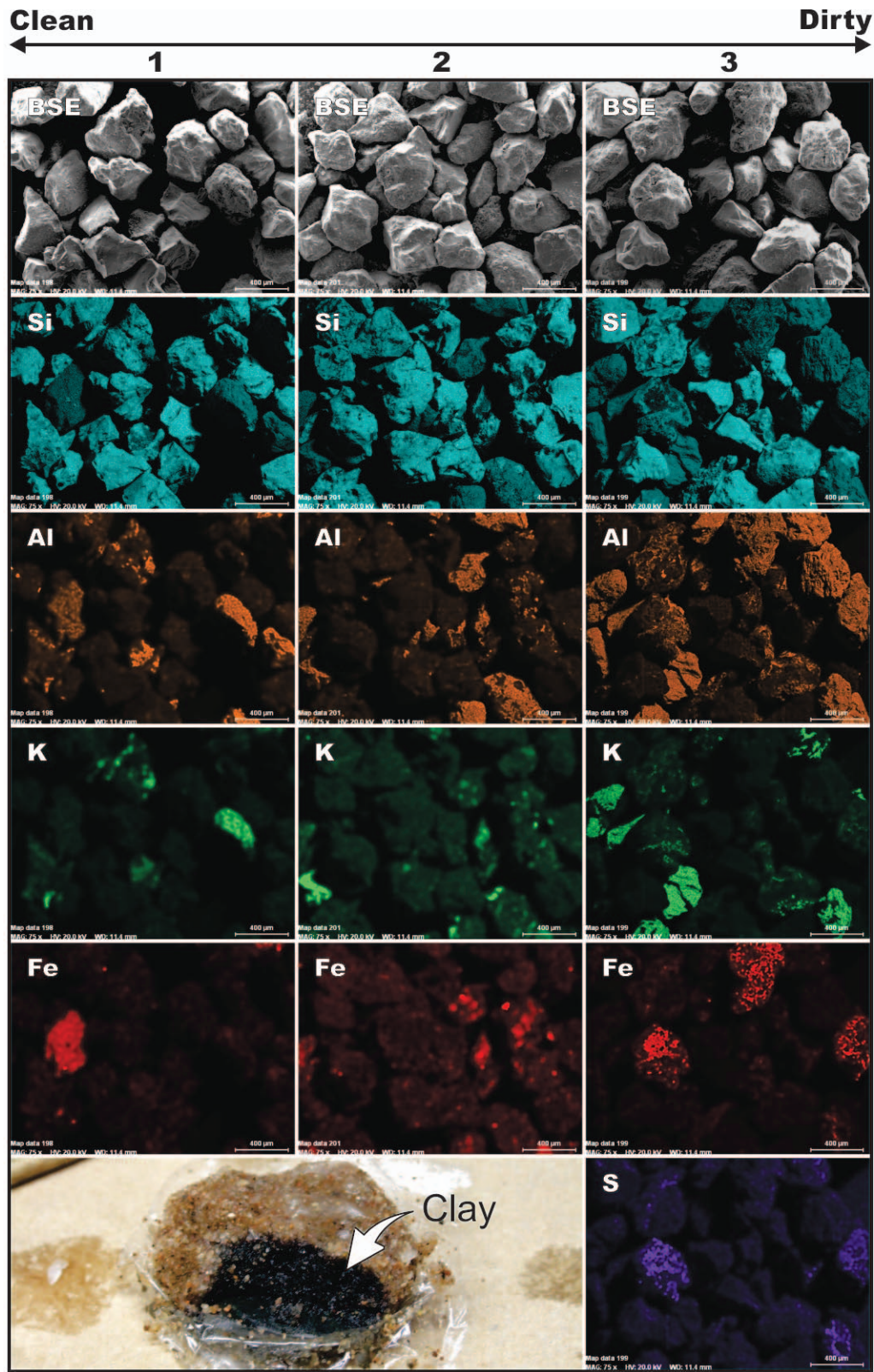


**FIGURE 4**—Elemental Mapping: ESEM-EDS analyses and backscattered electron (BSE; z-contrast) imaging of clean (1) to dirty (3) samples of fine-grained sand. Clean sands were composed almost entirely of quartz. Dirty samples were collected in close proximity to the decayed larva within the distinct black ring. Dirty grains are coated progressively by a milieu of aluminosilicate elements (Al-K-Fe mapped here). In addition, these grains also revealed the likely presence of iron sulfide (mapped for sample 3), potentially a precursor to the pyrite coatings proposed to accompany Ediacaran death-mask preservation (Gehling, 1999). The time series of grains shows that the Si X-ray signal dulls with a corresponding brightening of the Al signal. Bottom left: 3-dimensional black ring of clay-sized material precipitated around decaying carcass.

**TABLE 2**—Summary of primary elemental compositions (reported as mean normalized weight percentage  $\pm$  standard error) determined by ESEM-EDS point analyses (1 point per grain). Sample numbers: 1 = no precipitate (31 grains analyzed), 2 = intermediate precipitate (46 grains analyzed), and 3 = heavy precipitate (55 grains analyzed). Minor constituents observed but not reported here include Na, Cl, Mn, and Ti. See Supplementary Data 4<sup>1</sup> for complete analysis.

#	Si	O	C	Al	K	Mg	Ca	Fe	S
1	31.2 $\pm$ 2.0	49.5 $\pm$ 1.5	9.8 $\pm$ 2.2	3.6 $\pm$ 0.7	0.8 $\pm$ 0.3	0.7 $\pm$ 0.3	0.5 $\pm$ 0.3	1.7 $\pm$ 0.6	0.0 $\pm$ 0.0
2	28.5 $\pm$ 1.3	47.6 $\pm$ 1.7	8.1 $\pm$ 0.9	4.1 $\pm$ 0.7	1.7 $\pm$ 0.5	0.8 $\pm$ 0.2	1.2 $\pm$ 0.4	2.4 $\pm$ 0.7	0.3 $\pm$ 0.1
3	27.9 $\pm$ 1.2	51.1 $\pm$ 1.1	6.0 $\pm$ 0.7	5.8 $\pm$ 0.6	2.4 $\pm$ 0.6	0.7 $\pm$ 0.1	0.4 $\pm$ 0.1	1.8 $\pm$ 0.7	0.2 $\pm$ 0.1

## DISCUSSION AND CONCLUSIONS

### Experimental Support for the Microbial Death-Mask Hypothesis

Our results provide experimental support for Gehling's (1999) microbial death-mask model. There is a clear correlation between the presence of organic matter in the sand used to bury the organism, the formation of a black precipitate as a ring around the decaying carcass and, ultimately, the fidelity of preservation (Fig. 2). The absence of a black precipitate in those experiments that used sand cleaned of organic material (with the exception of just one sample at 2 weeks) confirms the importance of organic matter in the sediment to this type of preservation (also see Norris, 1989). Removing the organic material from the sand in Control 2 eliminated not only the microbial substrate but also the majority of microbes living on the surface of sediment grains. This slowed initial decay after burial, preventing both the swift generation of local anoxia (see Briggs and Kear, 1994) and cementation of grains required for fine-scale structural preservation (Gehling, 1999). In contrast, black rings formed in experiments with microbial mats within 1 day (and persisted for at least 6 weeks), likely reflecting both the high organic carbon content of the sediment, and the mat as a source of decay-promoting microbes. However, in control experiments using unsterilized sand, rings formed in 3 out of 4 experiments after 2 weeks, indicating that bacterial communities living on the surface of sediment grains, on the surface of larval cuticle, and in the gut of larvae likely also played a role. The disappearance of black rings over time reflects the slow diffusion of oxygen back into the vicinity of the carcass as decay slowed, causing dissipation/reoxygenation of the local microenvironment and reoxidation of reduced iron minerals (Sagemann et al., 1999; Martin et al., 2004). Gehling's (1999) model posited that the surface of storm beds was recolonized swiftly by mats, inhibiting the downward movement of oxygen and sulfate ions from the sediment-water interface and maintaining anaerobic conditions around the buried carcass. While no mat developed on the sediment surface over the 6-week duration of the experiment, the sheet of plastic film inserted to facilitate splitting may have inhibited vertical migration and surface colonization by the buried mat.

The fidelity of preservation is related to the concentration of organic matter (both the presence or absence of mats, and organic matter in the sand) and the formation of black rings. Fine-scale structures survived longer in experiments with microbial mats, where black rings also formed more consistently. Inferences based on taphonomic indices should, however, be viewed with caution: sampling was destructive and the dynamics of changing variables were not recorded. However, the consistency of results in replicate experiments (Fig. 2) suggests that our patterns are robust.

### Black Rings and Enhanced Preservation

The results of these experiments provide several explanations for the relationship between the formation of a black precipitate and enhanced fidelity of preservation.

1. ESEM imaging indicates that the black precipitate forms in association with an active biofilm coating the outside of sediment grains. ESEM-EDS analysis revealed evidence of likely iron sulfides, or at least spatially restricted associations of Fe and S, on the surfaces of grains in both samples 2 and 3 (Fig. 4), consistent with the microbial

death-mask model (Gehling, 1999), although pyrite framboids were not observed via electron imaging. However, the presence of iron sulfide is not extensive and there is little evidence to suggest that it forms a cement that would preserve fine-scale morphology. Microbial sealing, *sensu* Gehling (1999), and a longer period of decay may be required for the formation of a true pyritic death mask (Donald and Southam, 1999; Grimes et al., 2001).

2. Microbial populations derived from both mat and surrounding sand, which multiply in the vicinity of the carcass, may produce a significant volume of sediment-binding extracellular polymeric substance (EPS). The sediment trapping properties of EPS are well documented and may play a critical role in both micro- and regional-scale biosedimentary processes (see Riding, 2000). The generation of EPS additionally may be responsible for early cementation of grains and the retention of details of the organism. The role played by biofilms in stabilizing sediments and promoting mineral replication of tissues during decay has been emphasized by several authors (Briggs and Kear, 1994; Wilby et al., 1996; Briggs et al., 2005; McNamara et al., 2009). Our observation that sediment appeared to be caked around carcasses in experiments using mats (impeding the recovery of impressions) suggests that EPS derived from microbial blooms may trap and bind grains.

3. Both XPS and ESEM-EDS analyses revealed local elevations, either compositionally or proportionally, in the aluminosilicate elemental suite of Al, K, Fe, and Mg within the black precipitate surrounding the carcasses (Fig. 4, Table 2). While compositional variability undoubtedly exists in the natural sands, such variability is an unlikely explanation for the directional trends observed in the EDS data over the course of the experiment. Over time the sands showed: (1) higher concentrations of Al and K; (2) a higher proportion of grains with detectable Mg, Fe, and S; and (3) a corresponding decrease in the relative concentration of Si within the given electron beam interaction volume. While this should not be interpreted as a loss of Si from individual sand grains, we can infer that the EDS elemental maps captured a greater volume of the black coating per unit beam interaction volume as the experiments progressed. Although we did not observe the precipitation of true fine-grained clays, as such particles would have been revealed by electron imaging, our compositional data suggest a thicker aluminosilicate coating over time.

Martin et al. (2004) demonstrated the attachment of quartz and kaolinite to the surfaces of decaying lobster eggs in the presence of metabolizing bacteria; sediment was derived from the immediate environment and subsequently concentrated on the surfaces of eggs over several months of the experiment. Our results provide evidence that microbial activity may facilitate the precipitation of aluminosilicate minerals by concentrating aluminosilicate elemental constituents around decaying carcasses. If the generation of true clay minerals follows, then clay-sized particles generated around a carcass may serve to cast fine-scale morphology that otherwise might not be preservable given the coarser grain sizes of surrounding sediment. A layer of clay-sized particles would also provide a relatively impermeable barrier preventing oxygenated pore water from diffusing back to the vicinity of the carcass, and protecting pyrite from oxidation. Some support for this interpretation is provided by fossil material. Toporski et al. (2002) reported local enrichment of Al, Mg, S, Fe, and Ti in a fossilized biofilm from the Oligocene of Germany. Furthermore, Laflamme et al. (2011) reported the occurrence of nearly identical elemental consortia to

those in our experiments associated with *Aspidella* discs from the Avalon Peninsula where aluminosilicates are concentrated in a distinct fine-grained sediment layer surrounding holdfasts. Mapstone and McIlroy (2006) discovered concentrations of illite, chlorite, and smectite on hyporelief surfaces of discoidal fossils from the Neoproterozoic of central Australia, although they interpreted them as the result of background and fair-weather sedimentation, rather than as *in situ* precipitates related to decay. Similar associations of clay minerals and pyrite have been documented from carbonaceous compression-type Ediacaran microfossils from the Doushantuo and Denying Formations of South China (Anderson et al., 2011). Such observations suggest a common theme within multiple late Neoproterozoic and early Phanerozoic taphonomic windows.

#### Timing of Preservation

Our experiments suggest that formation of the black precipitate around a carcass may precede authigenic precipitation of iron sulfide and clay minerals, and furthermore, that the persistence of these black rings (and ultimately the development of a pyrite death mask) is dependent on the exclusion of oxygen. Experiments performed by Briggs and Kear (1993, 1994) and Sagemann et al. (1999) on shrimp demonstrated that the concentration of O<sub>2</sub> around a decaying carcass dropped to zero (complete anoxia) within 24 hours of death even in open conditions, but generally recovered to starting values within 10+ days (strongly dependant on the mass of individual carcasses), placing an upper temporal constraint on the mineralization of soft tissues. In our experiments, the expansion and contraction of the ring of black precipitate provides a proxy for the progress of anoxia and subsequent rediffusion of oxygen into the sediment surrounding the decaying larva. The time taken for oxygen to return to the carcass provides a constraint on the length of the preservational window. Black rings formed in experiments using microbial mats after 1 day, reached a maximum after 2 weeks, and virtually disappeared by 6 weeks. Thus it appears that 6 weeks would represent an upper limit for microbial mats to recolonize the surfaces of storm beds in order to prevent diffusion of oxygen back toward a decaying carcass and allow a death mask to form, at least in the particular conditions represented in our experiments. This window is considerably shorter in depositional settings lacking microbial mats (see C1 experiments), and pyritized death masks are less likely to form where organic matter is absent (C2 experiments).

It is unlikely that the cuticle of Ediacaran organisms was identical to that of *G. mellonella*. Although molecular studies support an Ediacaran age for Ecdysozoa (Wheeler et al., 2009; Erwin et al., 2011), there is little evidence for the presence of chitinous exoskeletons prior to the Cambrian (Miller, 1991). Chitin is a complex structural polysaccharide that is resistant to decay when complexed with protein in invertebrate cuticles (Baas et al., 1995; Flannery et al., 2001; Gupta et al., 2006). Under laboratory conditions Stankiewicz et al. (1998) demonstrated no structural degradation in chitin before decay had proceeded for 8 weeks, although considerable chemical changes occurred after 1 to 2 weeks. A placozoan affinity for the Ediacaran taxon *Dickinsonia* (as proposed by Sperling and Vinther, 2010) would suggest a considerably more labile integument. Our experiments using *G. mellonella* likely provide an upper limit for the formation of a death mask, although the persistence of anoxia around the carcass due to microbial sealing (not simulated in our experiments, and an important component of Gehling's [1999] model) would have extended mineralization.

Another limitation of our experiments is the use of fresh-water rather than marine mats to perform our experiments. The formation of pyrite death masks in the Ediacaran was presumably influenced by local concentrations of seawater sulfate. Modern, naturally occurring fresh water is typically sulfate-limited, and the water used in our experiments was particularly sulfate poor (~0.6 mM, see Supplementary Data 3<sup>1</sup>). However, evidence of sulfur isotope records (Kah et al.,

2004; Fike et al., 2006) and iron chemistry (Li et al., 2010) indicate that marine sulfate levels were low in the Neoproterozoic (as low as 0.2 mM in the Marinoan; Melezhik et al., 2005), and may have remained low until the upper Cambrian (2–12 mM; Gill et al., 2010). Our experiments simulated sulfate levels at the low end of ranges estimated for the Ediacaran, and provide evidence for the precipitation of iron sulfide despite extremely low SO<sub>4</sub>. The effect of sulfate concentrations on the formation of pyrite death masks remains to be investigated experimentally.

Our decay experiments support the basic tenets of the death-mask hypothesis and highlight the necessity for large amounts of organic matter (in the form of microbial mats) and anoxic conditions to allow the formation of external molds in coarse sediments. The rapid precipitation of aluminosilicate and iron sulfide precursors provides a taphonomic and diagenetic pathway allowing for the early lithification of sediment surrounding decaying organisms. The Ediacaran sedimentary regime, dominated by large expanses of microbial mats and an absence of destructive vertical burrowing, can explain the extensive preservation of relief impressions in Ediacaran sandstones worldwide.

#### ACKNOWLEDGMENTS

We thank L. Stout for construction of clone libraries and sequencing of our microbial mats, and H. Ernstberger for performing water chemistry analyses. R. Blake, M. Casey, D. Erwin, S. Gabbott, T. Hegna, J. Hunter, M. Purnell, L. Rochas, R. Sansom, and A. Wallace provided valuable assistance and discussion. Reviews by E. Sperling (Harvard University) and an anonymous reviewer improved a previous version of this manuscript. This work was supported by the Yale Peabody Museum of Natural History. JDS acknowledges support from the Virginia Tech Institute of Critical Technology and Applied Science. ML acknowledges generous support from the Natural Sciences and Engineering Research Council of Canada (NSERC), a Bateman Postdoctoral Fellowship, and a Smithsonian Institution Postdoctoral Fellowship.

#### REFERENCES

- ANDERSON, E.P., SCHIFFBAUER, J.D., and XIAO, S., 2011, Taphonomic study of Ediacaran organic-walled fossils confirms the importance of clay minerals and pyrite in Burgess Shale-type preservation: *Geology*, v. 39, p. 643–646.
- ALLISON, P.A., 1988, The decay and mineralization of proteinaceous macrofossils: *Paleobiology*, v. 14, p. 139–154.
- BAAS, M., BRIGGS, D.E.G., VAN HEEMST, J.D.H., KEAR, A.J., and DE LEEUW, J.W., 1995, Selective preservation of chitin during the decay of shrimp: *Geochimica et Cosmochimica Acta*, v. 59, p. 945–951.
- BRIGGS, D.E.G., 1995, Experimental taphonomy: *PALAIOS*, v. 10, p. 539–550.
- BRIGGS, D.E.G., 2003, The role of decay and mineralization in the preservation of soft-bodied fossils: *Annual Review of Earth and Planetary Sciences*, v. 31, p. 275–301.
- BRIGGS, D.E.G., and KEAR, A.J., 1993, Fossilization of soft tissue in the laboratory: *Science*, v. 259, p. 1439–1444.
- BRIGGS, D.E.G., and KEAR, A.J., 1994, Decay and mineralization of shrimps: *PALAIOS*, v. 9, p. 431–456.
- BRIGGS, D.E.G., MOORE, R.A., SHULTZ, J.W., and SCHWEIGERT, G., 2005, Mineralization of soft-part anatomy and invading microbes in the horseshoe crab *Mesolimulus* from the Upper Jurassic Lagerstätte of Nusplingen, Germany: *Proceedings of the Royal Society B*, v. 272, p. 627–632.
- BRUTON, D.L., 1991, Beach and laboratory experiments with the jellyfish *Aurelia* and remarks on some fossil “medusoid” traces, in Simonetta, A.M., and Conway Morris, S., eds., *The Early Evolution of Metazoa and the Significance of Problematic Taxa*: Cambridge University Press, Cambridge, UK, p. 125–129.
- CALLOW, R.H.T., and BRASIER, M.D., 2009, Remarkable preservation of microbial mats in Neoproterozoic siliciclastic settings: Implications for Ediacaran taphonomic models: *Earth-Science Reviews*, v. 96, p. 207–219.
- CLAPHAM, M.E., NARBONNE, G.M., and GEHLING, J.G., 2003, Paleocology of the oldest known animal communities: Ediacaran assemblages at Mistaken Point, Newfoundland: *Paleobiology*, v. 29, p. 527–544.

- COLE, J.R., WANG, Q., CARDENAS, E., FISH, J., CHAI, B., FARRIS, R.J., KULAM-SYED-MOHIDEEN, A.S., MCGARRELL, D.M., MARSH, T., GARRITY, G.M., and TIEDJE, J.M., 2009, The Ribosomal Database Project: Improved alignments and new tools for rRNA analysis: *Nucleic Acids Research*, v. 37, Database issue, p. D141–D145.
- DONALD, R., and SOUTHAM, G., 1999, Low temperature anaerobic bacterial diagenesis of ferrous monosulphide to pyrite: *Geochimica et Cosmochimica Acta*, v. 63, p. 2019–2023.
- DROSER, M.L., GEHLING, J.G., and JENSON, S., 2006, Assemblage palaeoecology of the Ediacara biota: The unabridged edition?: *Palaeogeography, Palaeoclimatology, Palaeoecology*, v. 232, p. 131–147.
- ERWIN, D.H., LAFLAMME, M., TWEEDT, S.M., SPERLING, E.A., PISANI, D., and PETERSON, K.J., 2011, The Cambrian conundrum: Early divergence and later ecological success in the early history of animals: *Science*, v. 334, p. 1091–1097.
- FEDONKIN, M.A., and WAGGONER, B.M., 1997, The Late Precambrian fossil *Kimberella* is a mollusc-like bilaterian organism: *Nature*, v. 388, p. 868–871.
- FIKE, D.A., GROTZINGER, J.P., PRATT, L.M., and SUMMONS, R.E., 2006, Oxidation of the Ediacaran ocean: *Nature*, v. 444, p. 744–747.
- FLANNERY, M.B., STOTT, A.W., BRIGGS, D.E.G., and EVERSHERD, R.P., 2001, Chitin in the fossil record: Identification and quantification of d-glucosamine: *Organic Geochemistry*, v. 32, p. 745–754.
- GEHLING, J.G., 1991, The case for Ediacaran fossil roots to the metazoan tree: *Geological Society of India Memoir*, v. 20, p. 181–224.
- GEHLING, J.G., 1999, Microbial mats in terminal Proterozoic siliciclastics: Ediacaran death masks: *PALAIOS*, v. 14, p. 40–57.
- GEHLING, J.G., 2000, Environmental interpretation and a sequence stratigraphic framework for the terminal Proterozoic Ediacara Member within the Rawnsley Quartzite, South Australia: *Precambrian Research*, v. 100, p. 65–95.
- GEHLING, J.G., DROSER, M.L., JENSEN, S., and RUNNEGAR, B.N., 2005, Ediacaran organisms: Relating form to function, in Briggs, D.E.G., ed., *Evolving Form and Function: Fossils and Development, Proceedings of a Symposium Honoring Adolf Seilacher for his Contributions to Paleontology in Celebration of his 80th Birthday*: Peabody Museum of Natural History, Yale University, New Haven, Connecticut, p. 43–67.
- GILL, B.C., LYONS, T.W., YOUNG, S.A., KUMP, L.R., KNOLL, A.H., and SALTZMAN, M.R., 2010, Geochemical evidence for widespread euxinia in the Later Cambrian ocean: *Nature*, v. 469, p. 80–83.
- GLAESSNER, M.F., and WADE, M., 1966, The late Precambrian fossils from Ediacara, South Australia: *Palaeontology*, v. 9, p. 599–628.
- GRAZHDANKIN, D., 2004, Patterns of distribution in the Ediacaran biotas: Facies versus biogeography and evolution: *Paleobiology*, v. 30, p. 203–221.
- GRAZHDANKIN, D., and GERDES, G., 2007, Ediacaran microbial colonies: *Lethaia*, v. 40, p. 201–210.
- GRIMES, S.T., BROCK, F., RICKARD, D., DAVIES, K.L., EDWARDS, E., BRIGGS, D.E.G., and PARKES, R.J., 2001, Understanding fossilization: Experimental pyritization of plants: *Geology*, v. 29, p. 123–126.
- GUPTA, S.C., LEATHERS, T.D., EL-SAYED, G.N., and IGNOFFO, C.M., 1992, Insect cuticle-degrading enzymes from the entomogenous fungus *Beauveria bassiana*: *Experimental Mycology*, v. 16, p. 132–137.
- GUPTA, S.C., LEATHERS, T.D., EL-SAYED, G.N., and IGNOFFO, C.M., 1994, Relationships among enzyme activities and virulence parameters in *Beauveria bassiana* infections of *Galleria mellonella* and *Trichoplusia ni*: *Journal of Invertebrate Pathology*, v. 64, p. 13–17.
- GUPTA, N.S., MICHELS, R., BRIGGS, D.E.G., EVERSHERD, R.P., and PANCOST, R.D., 2006, The organic preservation of fossil arthropods: An experimental study: *Proceedings of the Royal Society B*, v. 273, p. 2777–2783.
- GUPTA, N.S., CAMBRA-MOO, O., BRIGGS, D.E.G., LOVE, G.D., FREGENAL-MARTINEZ, M.A., and SUMMONS, R.E., 2008, Molecular taphonomy of microfossils from the Cretaceous Las Hoyas Formation, Spain: *Cretaceous Research*, v. 29, p. 1–8.
- HAGADORN, J.W., and BOTTJER, D.J., 1997, Wrinkle structures: Microbially mediated sedimentary structures in siliciclastic settings at the Proterozoic-Phanerozoic transition: *Geology*, v. 25, p. 1047–1050.
- KAH, L.C., LYONS, T.W., and FRANK, T.D., 2004, Low marine sulphate and protracted oxygenation of the Proterozoic biosphere: *Nature*, v. 431, p. 834–838.
- LAFLAMME, M., and NARBONNE, G.M., 2008, Ediacaran fronds: *Palaeogeography, Palaeoclimatology, Palaeoecology*, v. 258, p. 162–179.
- LAFLAMME, M., SCHIFFBAUER, J.D., NARBONNE, G.M., and BRIGGS, D.E.G., 2011, Microbial biofilms and the preservation of the Ediacara biota: *Lethaia*, v. 44, p. 203–213.
- LAFLAMME, M., SCHIFFBAUER, J.D., and NARBONNE, G.M., 2012, Deep-water microbially induced sedimentary structures (MISS) in deep time: The Ediacaran fossil *Iveshedia*, in Noffke, N.K., and Chafetz, H., eds., *Microbial Mats in Siliciclastic Depositional Systems Through Time*: SEPM Special Publication No. 101, p. 111–123.
- LI, C., LOVE, G.D., LYONS, T.W., FIKE, D.A., SESSIONS, A.L., and CHU, X., 2010, A stratified redox model for the Ediacaran ocean: *Science*, v. 328, p. 80–83.
- LIU, A.G., MCILROY, D., ANTCLIFFE, J.B., and BRASIER, M.D., 2011, Effaced preservation in the Ediacara biota and its implications for the early macrofossil record: *Palaeontology*, v. 54, p. 607–630.
- MAPSTONE, N.B., and MCILROY, D., 2006, Ediacaran fossil preservation: Taphonomy and diagenesis of a discoid biota from the Amadeus Basin, central Australia: *Precambrian Research*, v. 149, p. 126–148.
- MARTIN, D., BRIGGS, D.E.G., and PARKES, R.J., 2004, Experimental attachment of clay minerals to invertebrate eggs and the preservation of soft-bodied fossils: *Journal of the Geological Society, London*, v. 161, p. 735–738.
- MCNAMARA, M., ORR, P.J., KEARNS, S.L., ANADÓN, P., ALCALÁ, L., and PEÑALVER-MOLLÁ, E., 2009, Soft tissue preservation in Miocene frogs from Libros (Spain): Insights into the genesis of decay microenvironments: *PALAIOS*, v. 24, p. 104–117.
- MELEZHUK, V.A., FALICK, A.E., and POKROVSKY, B.G., 2005, Enigmatic nature of thick sedimentary carbonates depleted in  $^{13}\text{C}$  beyond the canonical mantle value: The challenges to our understanding of the terrestrial carbon cycle: *Precambrian Research*, v. 137, p. 131–165.
- MILLER, R.F., 1991, Chitin paleoecology: *Biochemical Systematics and Ecology*: v. 19, p. 401–411.
- MİYATA, S., CASEY, M., FRANK, D.W., AUSUBEL, F.M., and DRENKARD, E., 2003, Use of the *Galleria mellonella* caterpillar as a model host to study the role of the Type III secretion system in *Pseudomonas aeruginosa* pathogenesis: *Infection and Immunity*, v. 71, p. 2404–2413.
- NARBONNE, G.M., 1998, The Ediacara biota: A terminal Neoproterozoic experiment in the evolution of life: *GSA Today*, v. 8, p. 1–6.
- NARBONNE, G.M., 2004, Modular construction of early Ediacaran complex life forms: *Science*, v. 305, p. 1141–1144.
- NARBONNE, G.M., 2005, The Ediacara biota: Neoproterozoic origin of animals and their ecosystems: *Annual Review of Earth and Planetary Sciences*, v. 33, p. 421–442.
- NARBONNE, G.M., LAFLAMME, M., GREENTREE, C., and TRUSLER, P., 2009, Reconstructing a lost world: Ediacaran rangeomorphs from Spaniard's Bay, Newfoundland: *Journal of Paleontology*, v. 83, p. 503–523.
- NORRIS, R.D., 1989, Cnidarian taphonomy and affinities of the Ediacara biota: *Lethaia*, v. 22, p. 381–393.
- RETALLACK, G.J., 1994, Were the Ediacaran fossils lichens?: *Paleobiology*, v. 20, p. 523–544.
- RIDING, R., 2000, Microbial carbonates: The geological record of calcified bacterial-algal mats and biofilms: *Sedimentology*, v. 47, p. 174–214.
- SAGEMANN, J., BALE, S.J., BRIGGS, D.E.G., and PARKES, R.J., 1999, Controls on the formation of authigenic minerals in association with decaying organic matter: An experimental approach: *Geochimica et Cosmochimica Acta*, v. 63, p. 1083–1095.
- SAMINAKOVA, A., MISIKOVA, S., and LEOPOLD, J., 1971, Action of enzymatic systems of *Beauveria bassiana* on the cuticle of the greater wax moth larvae (*Galleria mellonella*): *Journal of Invertebrate Pathology*, v. 18, p. 322–330.
- SANSOM, R.S., GABBOTT, S.E., and PURNELL, M.A., 2010, Non-random decay of chordate characters causes bias in fossil interpretation: *Nature*, v. 463, p. 797–800.
- SEILACHER, A., 1984, Late Precambrian and Early Cambrian metazoans: Preservation or real extinctions?, in Holland, H.D., and Trendall, A.F., eds., *Patterns of Change in Earth Evolution*, (Dahlem Konferenzen): Springer-Verlag, Berlin, p. 159–168.
- SEILACHER, A., 1989, Vendozoa: Organismic construction in the Proterozoic biosphere: *Lethaia*, v. 22, p. 229–239.
- SEILACHER, A., 1992, Vendobionta and Psammocorallia: Lost constructions of Precambrian evolution: *Journal of the Geological Society, London*, v. 149, p. 607–613.
- SEILACHER, A., REIF, W.-E., and WESTPHAL, F., 1985, Sedimentological, ecological and temporal patterns of fossil Lagerstätten: *Philosophical Transactions of the Royal Society of London*, v. 311, p. 5–23.
- SERLING, E.A., and VINTNER, J., 2010, A placozoan affinity for *Dickinsonia* and the evolution of late Proterozoic metazoan feeding modes: *Evolution and Development*, v. 12, p. 201–209.
- SERLING, E.A., PISANI, D., and PETERSON, K.J., 2007, Poriferan paraphyly and its implications for Precambrian paleobiology: *Geological Society of London Special Publication*, v. 286, p. 355–368.
- SRIGG, R.C., 1949, Early Cambrian “Jellyfishes” of Ediacara, South Australia, and Mt. John, Kimberley District, Western Australia: *Transactions of the Royal Society of South Australia*, v. 73, p. 72–99.
- STANKIEWICZ, B.A., MASTALERZ, M., HOFF, C.H.J., BIERSTEDT, A., FLANNERY, M.B., BRIGGS, D.E.G., and EVERSHERD, R.B., 1998, Biodegradation of the chitin-protein complex in crustacean cuticle: *Organic Geochemistry*, v. 28, p. 67–76.
- STEINER, M., and REITNER, J., 2001, Evidence of organic structures in Ediacara-type fossils and associated microbial mats: *Geology*, v. 29, p. 1119–1122.
- TOPORSKI, J.K.W., STEELE, A., WESTALL, F., AVCI, R., MARTILL, D.M., and MCKAY, D.S., 2002, Morphologic and spectral investigation of exceptionally well-preserved bacterial biofilms from the Oligocene Enspel formation, Germany: *Geochimica et Cosmochimica Acta*, v. 66, p. 1773–1791.
- WHEELER, B.M., HEIMBERG, A.M., MOY, V.N., SPERLING, E.A., HOLSTEIN, T.W., HEBER, S., and PETERSON, K.J., 2009, The deep evolution of metazoan microRNAs: *Evolution and Development*, v. 11, p. 50–68.

- WILBY, P.R., BRIGGS, D.E.G., BERNIER, P., and GAILLARD, C., 1996, The role of microbial mats in the fossilization of soft tissues: *Geology*, v. 24, p. 787–790.
- WILBY, P.R., CARNEY, J.N., and HOWE, M.P.A., 2011, A rich Ediacaran assemblage from eastern Avalonia: Evidence of early widespread diversity in the deep ocean: *Geology*, v. 39, p. 655–658.
- WOOD, D.A., DALRYMPLE, R.W., NARBONNE, G.M., GEHLING, J.G., and CLAPHAM, M.E., 2003, Paleoenvironmental analysis of the late Neoproterozoic Mistaken Point and Trepassey formations, southeastern Newfoundland: *Canadian Journal of Earth Sciences*, v. 40, p. 1375–1391.
- XIAO, S., and LAFLAMME, M., 2009, On the eve of animal radiation: Phylogeny, ecology, and evolution of the Ediacara biota: *Trends in Ecology and Evolution*, v. 24, p. 31–40.

ACCEPTED NOVEMBER 21, 2011